

Review of Internal Solitary Waves

Xiangming Yu

1 Abstract

A variety of waves can be generated in the region between two fluids of different densities. These so called internal waves are dispersive and nonlinear even for modest amplitudes. This paper provides an review of various models (from weakly to fully nonlinear) of internal waves in the density-stratified flows. The properties of these waves as well as the processes of generation, interaction and transformation are discussed. In addition, interesting and curious phenomena in internal waves: leap-frogging solitary waves in a three-layered stratified flow are studied.

2 Introduction

The waves propagating on the boundary between two layers of fluids with different densities have been well studied and explained by particle motion under the action of gravity and inertial forces. The familiar example of such waves is the surface water waves (e.g. wind waves, swells, tsunamis) in seas and oceans. On the other hand, the density and shear flow in the ocean and atmosphere are stratified in the vertical direction, such that so called internal waves can propagate at various depths in the ocean and at various heights in the atmosphere. The weak density variations in the ocean and atmosphere causes weak restoring forces, and the amplitudes of natural internal waves can be achieved, significantly exceeding the limiting amplitudes of the waves on the sea-air boundary. 1 shows an example of an observed large amplitude (up to 40 m) long internal waves in the North Atlantic to the north of Ireland (Small et al. 1999 [15]). The fact that they do not break and remain of finite amplitude for long distances implies that dispersion is not dominant.

This paper summarizes both weakly and fully nonlinear models of steady-state internal solitary waves in section 1. The extended KdV (eKdV) equation with cubic nonlinearity is the most common weakly nonlinear model for internal waves. In addition eKdV is also adopted as the phenomenological model of choice for fully nonlinear model. In section 2, the phenomena of leap-frogging solitary waves are discussed. Both analytical and experimental results are presented.

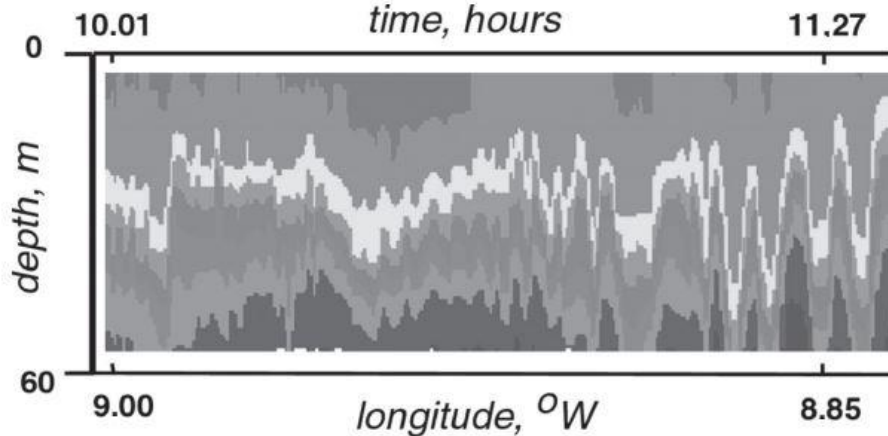


Figure 1: A group of intense internal waves observed in the Atlantic, near Ireland (Small et al. 1999)

3 Models for Internal Solitary Waves

3.1 Weakly Nonlinear Models

Despite of the high nonlinearity of observed internal waves in the ocean, weakly nonlinear KdV-type theories have played an significant role in modeling these waves, if not always the precise quantitative details. Helfrich and Melville (2006) [5] point out that they have the advantage of permitting modeling of unsteady wave evolution under various conditions with a reduced wave equation. The KdV equation is derived based on an assumption that nonlinearity, scaled by $\alpha = a/H$, and dispersion, $\beta = (H/l)^2$, are comparable and small.

$$\beta = o(\alpha) \ll 1 \tag{1}$$

where a is a measure of wave amplitude, H is an intrinsic vertical scale, and l is a measure of wavelength. Weakly nonlinear theories for infinitely deep fluids can be found in Benjamin (1967) [1] and Ono (1975) [13], or intermediate depth can be found in Joseph (1977) [6] and Kubota et al. (1978) [17].

A useful variant of the KdV equation is the extended KdV (eKdV) equation with cubic nonlinearity (Lee & Beardsley 1974 [8], and Djordjevic & Redekopp 1978 [3]):

$$\eta_t + (c_0 + \alpha_1\eta + \alpha_2\eta^2)\eta_x + \beta_1\eta_{xxx} = 0 \tag{2}$$

where $\eta(x, t)$ is the isopycnal vertical displacement, and x is the spatial variable in the direction of wave propagation. The three coefficients α_1 , α_2 , and β_1 are related to the steady background stratification and shear flows. c_0 is the linear phase speed.

$$\begin{aligned}
c_0 &= \left(\frac{g\sigma b_1 b_2}{b_1 + b_2} \right)^{1/2} \\
\alpha_1 &= 3/2 c_0 \frac{b_1 - b_2}{b_1 b_2} \\
\alpha_2 &= \frac{3c_0}{(b_1 b_2)^2} \left[\frac{7}{8} (b_1 - b_2)^2 - \left(\frac{b_2^3 + b_1^3}{b_1 + b_2} \right) \right] \\
\beta_1 &= \frac{c_0}{6} b_1 b_2
\end{aligned} \tag{3}$$

where g is the gravity, $\sigma = 2(\rho_2 - \rho_1)/(\rho_1 + \rho_2) \ll 1$ is the relative layer density difference, ρ_1 and ρ_2 are densities of the upper and lower layers, and b_1 and b_2 are the mean upper and lower layer depths, respectively.

The solutions to the eKdv (equation 2) are given (Kakutani & Yamasaki 1978 [7], Miles 1979 [11], Ostrovsky & Stepanyants 1989 [14])

$$\eta = \frac{\eta_0}{b + (1 - b) \cosh^2 \gamma(x - ct)} \tag{4}$$

where

$$\begin{aligned}
c &= c_0 + \frac{\eta_0}{3} \left(\alpha_1 + \frac{1}{2} \alpha_2 \eta_0 \right) \\
\gamma^2 &= \frac{\eta_0 (\alpha_1 + \frac{1}{2} \alpha_2 \eta_0)}{12\beta} \\
b &= \frac{-\eta_0 \alpha_2}{2\alpha_1 + \alpha_2 \eta_0}
\end{aligned} \tag{5}$$

Equation 2 becomes KdV equation when α_2 is set to zero, and the classical *sech*² solution is obtained from equation 4. The wavelength, $\lambda |\eta_0|^{-1/2}$, decreases with increasing amplitude. Thus, this solution cannot capture the broadening of waves in figure 2 [4]. The heavy dash line is the wave profile predicted by the KdV equation using the background stratification. On the other hand, solitary waves described by eKdV can capture the broadening shape when $\alpha_2 < 0$ ($0 < b < 1$). As KdV solutions do, small amplitude waves become narrower with increasing $|\eta_0|$. However, as b is approaching to 1 (upper limit), waves start to broaden until the maximum amplitude $\eta_0 = -\alpha_1/\alpha_2$ is reached. Figure 3 [5] shows a solitary wave solutions of the eKdV

equation 2 with a range of amplitudes for $\beta = \alpha_1 = -\alpha_2 = 1$ and $\eta_{0,max} = 1$. As expected, the maximum wave (at upper limit) becomes infinitely long and a board plateau that terminate at each end by dissipationless bores.

The coefficient of the cubic term α_2 can have either sign for more general background stratifications and shear flows. When it is positive, the broadening character and upper bound on wave amplitude do not exist, rather we can observe a minium wave amplitude $\eta_0 = -2\alpha_1/\alpha_2$ for $\alpha_1\eta_0$.

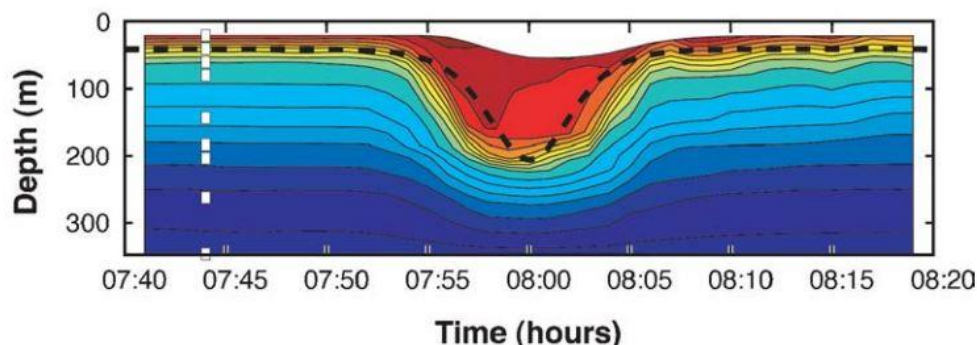


Figure 2: A single large wave in 340m of water in the northeast South China Sea (from Duda et al. 2004). The heavy dash line is the profile of a KdV solitary wave calculated using the background stratification.

3.2 Large Amplitude Models

The KdV-type theories based on weakly nonlinearity assumption have been found to be success to model waves even outside their formal range of validity. Stanton & Ostrovsky (1998) [16] found that eKdV well captures the characteristics of highly nonlinear waves. Therefore, eKdV has been taken as the phenomenological model of choice for highly nonlinear solitary waves.

Miyath (1988) [12] and Choi Camassa (1999) [2] extend the weakly nonlinear eKdV model to fully nonlinear model with $\alpha = o(1)$, while remaining only the first order weakly dispersive effects, $\beta \ll 1$. Relative to the solutions of the eKdV model, the solitary wave solutions of Miyata-Chi-Camassa (MCC) equations predict more broadening and slow wave shapes with increasing amplitude. This theory produces a maximum wave with amplitude $\eta_{0,max} = (b_1 - b_2)/2$ which has infinitely long wavelength. Figure compares the solutions of KdV, eKdV and MCC equations. Significant

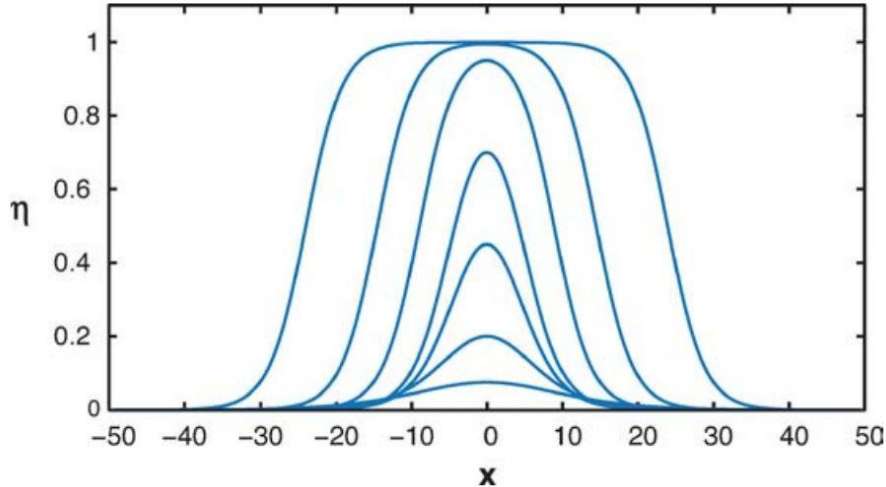


Figure 3: Solitary wave solutions of the eKdV equation 2 for arbitrary choice of the parameters $\beta = \alpha_1 = -\alpha_2 = 1$ (Helfrich and Melville 2006).

differences are observed between the eKdV and KdV solutions. For relatively small amplitude, however, differences between these two theories emerge. The comparison of the wave shapes and properties between eKdV and MCC shows that these two theories agree well for the range $0.4 < b_1/(b_1 + b_2) < 0.6$, where the scaling requirement for nonlinearity ($\alpha \ll 1$) of eKdV are approximately satisfied. Differences grow rapidly outside this range where nonlinearity starts to be significant. MCC solitary wave solutions show good agreement with experimental measurements (Choi & Camassa 1999 [2], and Michallet & Barthelemy 1998 [10]). One limitation of the MCC model is that solitary waves of sufficient amplitude could be unstable at high wave numbers t Kelvin-Helmholtz instability. For example, if a grid with too fine resolution is used for numerical calculation, unstable short waves will emerge near the wave crest and overwhelm the calculation.

Ostrovsky & Grue (2003) derived equations equivalent to MCC equations, but for strongly nonlinear dispersive waves ($\beta = o(1)$). They added nonlinear dispersive effects from the phenomenological derivation of the KdV equation.

$$\eta_t + c(\eta)\eta_x + (\beta(\eta)\eta_{xx})_x = 0 \quad (6)$$

where $c(\eta)$ is the exact nonlinear speed from the nondirective theory and

$$\beta(\eta) = \frac{1}{6}c(\eta)(b_1 + \eta)(b_2 - \eta) \quad (7)$$

The numerical solutions of solitary waves from their equations have properties that agree reasonably well with the MCC equations. And their equations avoid the instability issue found for the MCC equations.

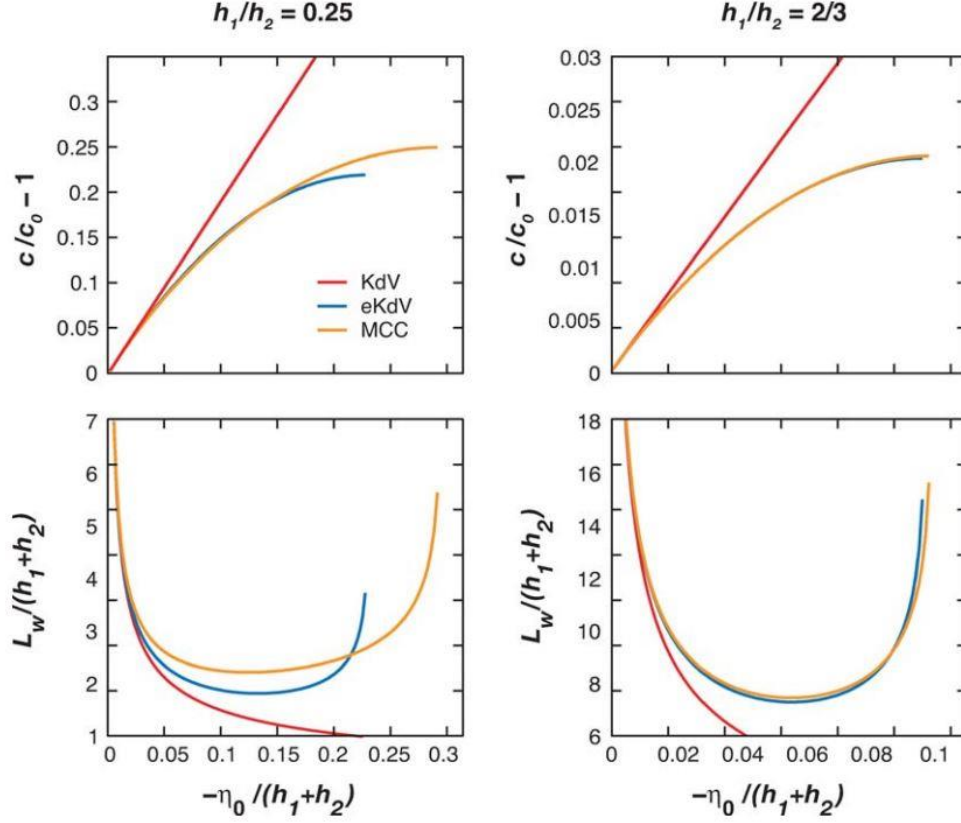


Figure 4: Comparison of solitary wave solutions of the KdV (red), eKdV (blue), and MCC (orange) theories. The top row shows the wave speed c vs. amplitude η_0 . The bottom row shows the wavelength L_w vs. amplitude η_0 . The comparison is done for two stratifications $b_1/b_2 = 1/4$ (left column) and $b_1/b_2 = 2/3$ (right column). For both the eKdV and MCC waves, the maximum wave amplitude corresponds to the end of the speed curves.

4 Leap-frogging Solitary Waves

4.1 Problem description

Let us consider a problem that two single-mode internal solitary waves propagate unidirectionally along vertically separated pycnoclines as shown in figure 5. Three homogeneous fluid layers of thickness H_1 , H_2 , and H_3 are separated by two thin layers of gradually changing density profiles. The thickness of these two layers $2h_1$ and $2h_2$ are small compared with the thickness of each fluid. Two internal solitary waves moves in these two thin layers with a relatively small difference in their phase speeds. Let us consider two limiting cases at first.

- Large separation between the density interfaces
The two solitary waves would propagate independently. The faster wave would overtake the slower one without energy exchange.
- Small separation between the density interfaces
The two interfaces would overlap with each other and form essentially a single pycnocline. In such a case, the interaction between the two solitary waves would be characterized by a single upstream energy transfer from the lagging wave to the leading wave as depicted in figure 6

The intermediate case that the pycnoclines are separated but not too far apart is our focus in this section. In this case, a new phenomenon can be found due to the coupling between the upper and lower solitary waves.

4.2 Results and Analysis

The analysis of Liu et al. (1980) [9] gives two coupled equations for the evolutions of the wave amplitudes $A(\xi, T)$ and $B(\xi, T)$ of single-mode, weakly nonlinear, long internal waves each in one pycnocline:

$$\begin{aligned} A_T + \alpha_1 A A_\xi - \beta_1 \frac{\partial^2}{\partial \xi^2} \mathfrak{H}_1(A) - \beta_1 \frac{\partial^2}{\partial \xi^2} \mathfrak{H}_2(B) &= 0 \\ B_T - \Delta C + \alpha_2 B B_\xi - \beta_2 \frac{\partial^2}{\partial \xi^2} \mathfrak{H}_3(B) - \beta_2 \frac{\partial^2}{\partial \xi^2} \mathfrak{H}_2(A) &= 0 \end{aligned} \tag{8}$$

where the operators \mathfrak{H}_1 , \mathfrak{H}_2 , and \mathfrak{H}_3 refer to Liu et al. (1980) [9]. The time T and spacial variable ξ are in a reference frame moving with the upper wave of speed C_0 . α and β are coefficients measuring the strength of nonlinearity and dispersion in each

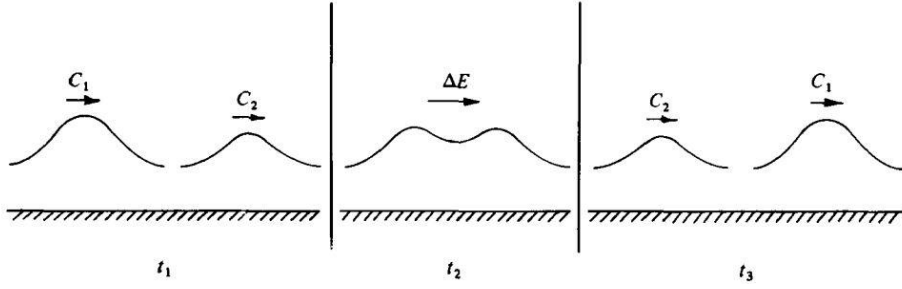


Figure 6: Sketch of the upstream energy transfer between free surface solitons traveling from left to right. The times t_1 , t_2 , and t_3 are successive instants before, at the middle of, and after the interaction, respectively.

observed in the experiment conducted by Weidman & Johnson (1982) as shown in figure 8. Figure 9 shows the measured evolution of the amplitude difference Δa_i between the two solitary waves as a function of time. The evolution of relative phase σ is presented in figure 10. Consistent with the prediction by the analytical analysis, Δa_i and σ are approximately 90° out of phase. In addition, both the amplitude and the period of the phase measurements in figure 10 are continuously increasing with time.

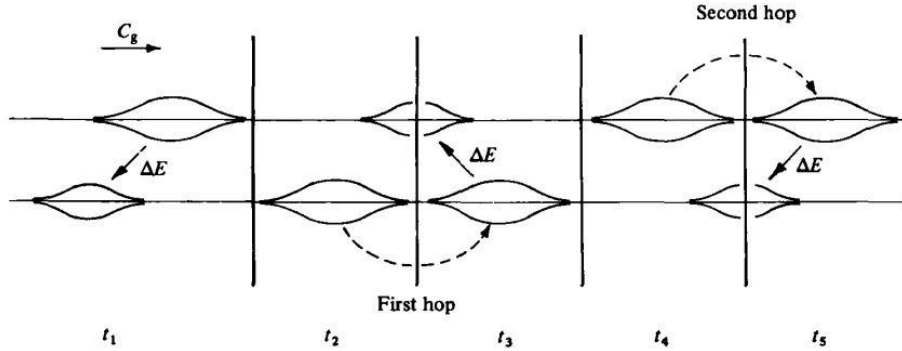


Figure 7: Sketch of the downstream energy transfer between two internal waves travelling along neighbouring pycnoclines. The wave is moving from left to right at the group velocity. The times t_1, \dots, t_5 denote successive times during the resonant cycle.

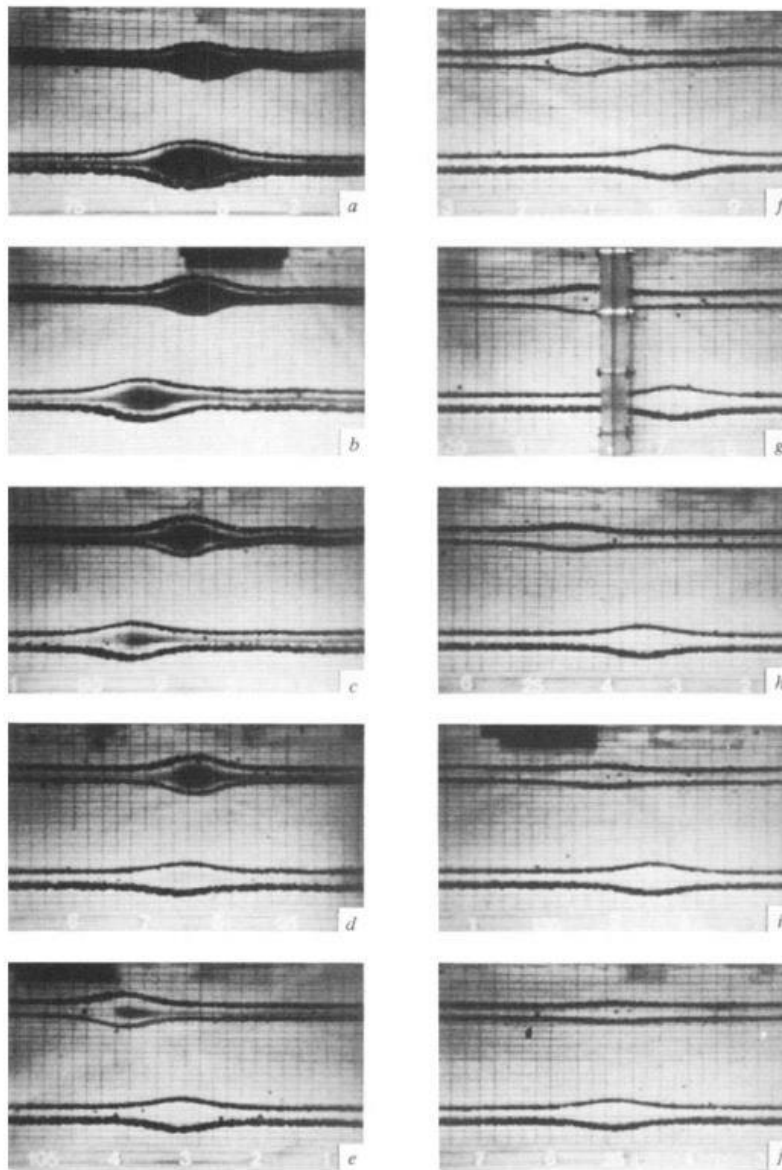


Figure 8: Photographic sequence exhibiting a solitary wave resonant interaction over one complete cycle. The waves propagate from right to left, and time increases from (a) to (j) with a constant time interval of 20s between frames (Weidman & Johnson 1982 [18]).

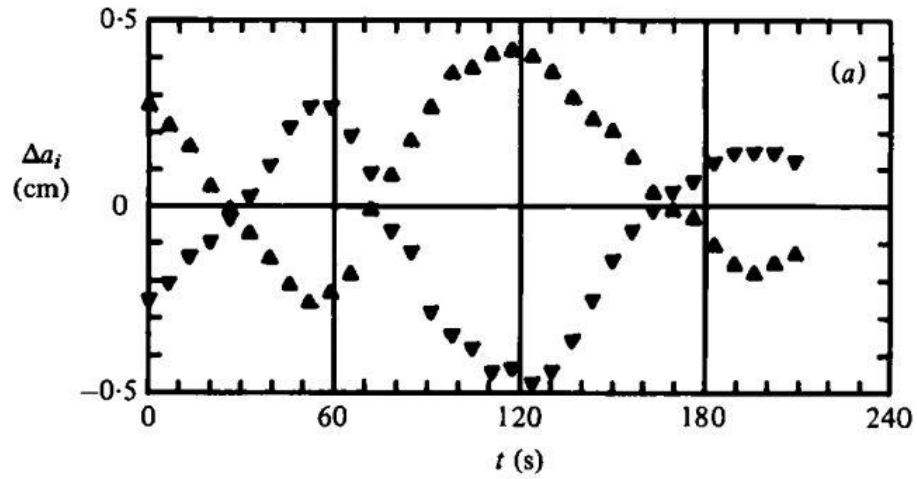


Figure 9: Evolution of the amplitude difference between the upper and lower solitary waves (Weidman & Johnson 1982 [18])

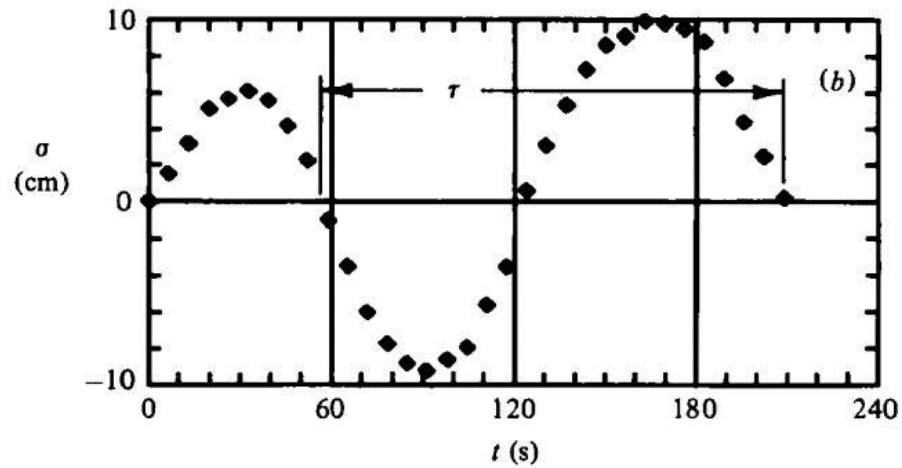


Figure 10: Evolution of the relative phase between the upper and lower solitary waves (Weidman & Johnson 1982 [18])

References

- [1] T Brooke Benjamin. Internal waves of permanent form in fluids of great depth. *Journal of Fluid Mechanics*, 29(03):559–592, 1967.

- [2] Wooyoung Choi and Roberto Camassa. Fully nonlinear internal waves in a two-fluid system. *Journal of Fluid Mechanics*, 396:1–36, 1999.
- [3] V Dj Djordjevic and LG Redekopp. The fission and disintegration of internal solitary waves moving over two-dimensional topography. *Journal of Physical Oceanography*, 8(6):1016–1024, 1978.
- [4] Timothy F Duda, James F Lynch, James D Irish, Robert C Beardsley, Steven R Ramp, Ching-Sang Chiu, Tswen Yung Tang, and Y-J Yang. Internal tide and nonlinear internal wave behavior at the continental slope in the northern south china sea. *Oceanic Engineering, IEEE Journal of*, 29(4):1105–1130, 2004.
- [5] Karl R Helfrich and W Kendall Melville. Long nonlinear internal waves. *Annu. Rev. Fluid Mech.*, 38:395–425, 2006.
- [6] RI Joseph. Solitary waves in a finite depth fluid. *Journal of Physics A: Mathematical and General*, 10(12):L225, 1977.
- [7] Tsunehiko Kakutani and Nobuyoshi Yamasaki. Solitary waves on a two-layer fluid. *Journal of the Physical Society of Japan*, 45(2):674–679, 1978.
- [8] Chi-Yuan Lee and Robert C Beardsley. The generation of long nonlinear internal waves in a weakly stratified shear flow. *Journal of Geophysical Research*, 79(3):453–462, 1974.
- [9] AK Liu, T Kubota, and DRS Ko. Resonant transfer of energy between non-linear waves in neighboring pycnoclines. *STUDIES IN APPLIED MATHEMATICS*, 63(1):25–45, 1980.
- [10] H Michallet and E Barthelemy. Experimental study of interfacial solitary waves. *Journal of Fluid Mechanics*, 366:159–177, 1998.
- [11] JOHN W MILES. On internal solitary waves. *Tellus*, 31(5):456–462, 1979.
- [12] Motoyasu Miyata. Long internal waves of large amplitude. In *Nonlinear Water Waves*, pages 399–406. Springer, 1988.
- [13] Hiroaki Ono. Algebraic solitary waves in stratified fluids. *Journal of the Physical Society of Japan*, 39(4):1082–1091, 1975.
- [14] LA Ostrovsky and Yu A Stepanyants. Do internal solitons exist in the ocean? *Reviews of Geophysics*, 27(3):293–310, 1989.

- [15] J Small, TC Sawyer, and JC Scott. The evolution of an internal bore at the malin shelf break. In *Annales Geophysicae*, volume 17, pages 547–565. Springer, 1999.
- [16] TP Stanton and LA Ostrovsky. Observations of highly nonlinear internal solitons over the continental shelf. *Geophysical Research Letters*, 25(14):2695–2698, 1998.
- [17] DRS Ko T. Kubota and LD Dobbs. Weakly-nonlinear, long internal gravity waves in stratified fluids of finite depth. *Journal of Hydronautics*, 12(4):157–165, 1978.
- [18] PD Weidman and M Johnson. Experiments on leapfrogging internal solitary waves. *Journal of Fluid Mechanics*, 122:195–213, 1982.